Environmental Science & Technology

Article

pubs.acs.org/est

Assessing Environmental Fate of β-HCH in Asian Soil and Association with Environmental Factors

Yue Xu,[†,‡] Chongguo Tian,[†,*] Jianmin Ma,[§] Gan Zhang,[‡] Yi-Fan Li,[§] Lili Ming,[‡] Jun Li,[‡] Yingjun Chen,[†] and Jianhui Tang[†]

[†]Laboratory of Coastal Zone Environmental Processes, Yantai Institute of Coastal Zone Research(YIC), Chinese Academy of Sciences (CAS); Shandong Provincial Key Laboratory of Coastal Zone Environmental Processes, YICCAS, Yantai Shandong 264003, China

[‡]State Key Laboratory of Organic Geochemistry, Guangzhou Institute of Geochemistry, Chinese Academy of Sciences, Guangzhou, 510640, China

[§]Air Quality Research Division, Science and Technology Branch, Environment Canada, 4905 Dufferin Street, Toronto, Ont, M3H 5T4, Canada

Supporting Information

ABSTRACT: Chinese Gridded Pesticide Emission and Residue Model was applied to simulate long-term environmental fate of β-HCH in Asia spanning 1948−2009. The model captured well the spatiotemporal variation of β-HCH soil concentrations across the model domain. β-HCH use in different areas within the model domain was simulated respectively to assess the influence of the different sources of β-HCH on its environment fate. A mass center of soil residue (MCSR) was introduced and used to explore environmental factors contributing to the spatiotemporal variation of β-HCH soil residue. Results demonstrate that the primary emission dominates β-HCH soil residues during the use of this pesticide. After phase-out of the pesticide in 1999, the change in β-HCH soil residues has been associated with the Asian summer monsoon, featured by northward displacement of the MCSR. The displacement from several major sources in China and northeastern Asia shows a downward trend at a 95% confidence level, largely caused by environmental degradation and northward delivery of β-HCH under cold condition in northern area. The MCSRs away from the India and southern and southeastern Asia sources show a rapid northward displacement at a 99% confidence level, featuring the cold trapping effect of the Tibetan Plateau.

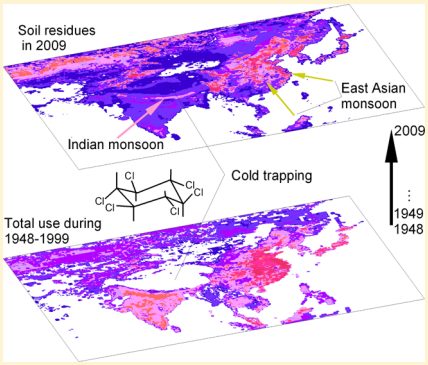

INTRODUCTION

Technical hexachlorocyclohexane (HCH) was one of the most widely used pesticides in the world during the second half of the 20th century. During this period, about 10 million tons of the pesticide were released into the environment.[1] Technical HCH is a mixture of several isomers in the proportions α: 60−70%, β: 5−12%, γ: 10−12%, δ: 6−10%, and ε: 3−4%.[2] All isomers of HCH are characterized by environmental persistence, toxicity, potential for bioaccumulation and long-range transport.[3] Due to increasing concern on environmental contamination, technical HCH has been phased-out or banned worldwide before the 2000s.[4] In 2009, α-HCH, β-HCH, and γ-HCH were added to Annex A of the Stockholm Convention on Persistent Organic Pollutants (POPs) with no exemptions for ongoing production.

Asia has been identified as a main source region of technical HCH in the world. China, the Former Soviet Union, and India together were estimated to consume about 75% of global total usage of the pesticide.[4] Although the use of technical HCH was discontinued in these countries and regions over 10 years ago, the environmental levels of HCH isomers were still high,[5,6] and posed a significant impact on ecosystems.[7] Presently, β-HCH is the predominant isomer in the environment[8] and human body[7] because of its resistance to microbial degradation and strong potential to bioaccumulate.[9]

Like other POPs, partitioning and exchange of β-HCH among environmental matrices are strongly affected by temperature.[10,11] The Tibetan Plateau, located in the center of Asia, is the highest and biggest plateau on Earth. The low temperature plays a very important role in regional cycling and distribution of POPs in the plateau as a result of the cold trapping effect.[12] Previous studies have demonstrated that HCH contamination in the Tibetan Plateau was largely attributed to the emission from Indian sources.[13,14] In addition, the Asian monsoon system, including Indian and East Asia monsoon subsystems, as an important large-scale atmospheric circulation system, has also been found to dominate

Received: May 21, 2012
Revised: August 7, 2012
Accepted: August 13, 2012
Published: August 13, 2012

atmospheric transport and regional cycling of POPs over Asia.[14,15] However, no comprehensive studies have been devoted to investigate the environmental fate of β-HCH in Asia under influence of regional environmental conditions before and after the phase-out of technical HCH. Here we investigate numerically the long-term environmental fate of β-HCH from 1948 to 2009 using Chinese Gridded Pesticide Emission and Residue Model (ChnGPERM). The present study pays special attention to soil residues of β-HCH across Asia because the spatial pattern of POPs in soils often exhibits stronger signatures of the long-term effect of environmental factors as compared with that in air,[16] and soil is a major storage compartment for β-HCH[3]. The main objectives are to identify temporal and spatial variations of β-HCH soil residues, track sources of soil residues, and examine the influence of the Asian monsoon and the cold trapping of the Tibetan Plateau on β-HCH fate in Asian environment.

MATERIALS AND METHODS

Model and Model Input. The ChnGPERM employed in this investigation has been used in previous numerical studies of α-HCH budget[16] and atmospheric outflow[17] from China. Briefly, the model consists of transfer and transport modules. The transfer module, using a level IV fugacity method,[18] describes concentration variation and intercompartmental transfer of a pesticide in the multimedia environments, including five soil types in four well-mixed levels, water, sediment, and air compartment in the atmospheric boundary layer (ABL, 0−1000 m). The five soil types are dry cropland, paddy field, forestry, grassland, and uncultured land. The depths of the four soil layers are 0.1, 1.0, 20, and 30 cm from top to bottom, respectively. The transport module, using a Lagrangian approach, solves horizontal, and vertical mass exchange of the chemical among different grid cells in the ABL and the atmospheric low troposphere (ALT, 1000−4000 m). The ChnGPERM was originally developed based on 1/6° latitude by 1/4° longitude resolution spanning 17−55°N and 70−135°E.[16] In the present study, it has been extended to a region spanning 0−60°N and 50−150°E with $^1/_4$° latitude by $^1/_4$° longitude resolution, as shown in the Supporting Information (SI) Figure S1. Given that there was no available geographical data on dry cropland and paddy field over the model domain, the two soil types were incorporated as cropland, and four soil types were considered in the present study. To better handle air-surface exchange and atmospheric transport of β-HCH, the ABL was separated into the atmospheric surface layer (0−100 m) and the planetary boundary layer (PBL, 100−1000 m). The detailed structure and physical/chemical processes included in the model are described elsewhere[16] and in the SI.

The environmental and geophysical data input in the model include daily meteorological data, land use, and soil characteristics. The meteorological data (winds, temperature, precipitation) from 1948 to 2009 at the ChnGPERM model grids of $^1/_4$° × $^1/_4$° latitude/longitude were interpolated, using the Canadian Meteorological Centre's objective analysis and interpolation system, from the daily objectively analyzed data from the United States National Center for Environmental Prediction (NCEP) reanalysis[19] with spatial spacing of 2.5° × 2.5° latitude/longitude. The gridded land use data (cropland, forestry, grassland, uncultured land and water) were derived from a MODIS production describing global land cover with $^1/_4$° × $^1/_4$° latitude/longitude resolution.[20] Based on the land cover, the gridded soil characteristic data (bulk density, organic carbon content, and porosity) were interpolated from a global soil data set with 1° latitude by 1° longitude resolution.[21]

A global usage inventory of technical HCH with 1° × 1° latitude/longitude from 1945 to 1999[22] was split into $^1/_4$° × $^1/_4$° latitude/longitude grids using the area ratios of cropland from the gridded land use data. The gridded inventory of β-HCH was created by assuming 8.5% composition of β-HCH in technical HCH.[2] SI Figure S1 shows spatial distribution of accumulated β-HCH usage with $^1/_4$° × $^1/_4$° latitude/longitude during 1945−1999 in the model domain. The processes of β-HCH entering into the environment during its application were assessed by application modes of technical HCH and cultivation activities in the model domain.[16] Two application modes, spray and seed treatment (which account for 85% and 15% of primary emissions of the pesticide), were considered here, respectively.[23] It has been assumed that technical HCH was directly emitted into the atmospheric surface layer and the first soil layer of cropland during the spray period, and discharged into the first three soil layers of cropland during the seed treatment period (details in the SI). The underlying assumption for the estimation was that primary emissions to air occurred mainly as a result of wind drift losses of droplets during pesticide spraying, rather than volatilization after application to soil. In contrast, secondary emissions from soil and water, which include volatilization as a function of chemical properties and temperature, were assessed by our model. The cultivation activities consist of single, double and triple cultivation, determined by the frost-free period and accumulated daily temperature ≥10 °C over the period of time.[24] SI Figure S2 displays averaged geographical pattern of the cultivation activities estimated by daily surface temperature from 1950 to 2000. The geographical pattern was used to determine the period during which technical HCH was applied. The periods for those application modes are listed on SI Table S4.

Since the meteorological data were available only from 1948 and the usage of technical HCH during 1945−1947 was less than 0.01% of the total usage from 1945 to 1999 in the model domain (SI Figure S3), the numerical simulations were performed successively from 1948 to 2009 at a time step of 1 day.

Numerical Experiment Setup. To identify quantitatively the relative contribution of different source of β-HCH to its budget, numerical simulations have been performed subject to five model scenarios. These five scenarios consist of (1) all source in the model domain, termed AS; (2) sources in the area north of 30°N excluding India and China, termed NS; (3) sources in China only, termed CS; (4) sources in India only, termed IS; and (5) source in the area south of 30°N excluding India and China, termed SS. The accumulated β-HCH usage of 1948 through 1999 in the model domain was 542 kilotons, in which 69 kilotons were used in the NS area, 344 kilotons in China, 90 kilotons in India, and 40 kilotons in the SS area (SI Figure S3). These usage values were obtained by summing the gridded usage over each source region, as illustrated by SI Figure S1. The five model scenarios were set up based on the source strength and locations, and the potential effects of meteorological conditions on the environmental fate of β-HCH over Asia. For example, China and India were the largest user of technical HCH in the world.[4] As aforementioned, regional cycling of the pesticide emitted from these two countries has

been associated with Indian monsoon and East Asian monsoon.[14,15] East Asian winter monsoon changes its direction from northwest to northeast near 30° N and the summer monsoon front lies also near this latitude in east China, as shown in SI Figure S4. Therefore, the atmospheric circulation system near 30°N in east China exhibits the strongest monsoon signatures. In addition, the major non-China/India source of β-HCH in Northeast Asia lies north of 30°N whereas the major non-China/India source in Southeast Asia lies south of 30°N (see SI Figure S1). To separate those non-China/India sources from China and India sources, we set up the model scenarios 2 and 5 in order to better understand the source-receptor relationships of β-HCH in Asia.

Mass Center and Statistical Analysis. The contribution of β-HCH emitted from each source to receptors in the model domain was assessed through calculating the ratios of the mass of β-HCH soil residue or atmospheric deposition from each scenario to the total mass summed over the model scenarios 2–5. The mass center of a body is defined as a point in space where the entire mass of the body is concentrated. It is often used for assessing spatial variation of the density of a body with time.[25,26] Given that the gridded soil residue can be referred to as geographical distribution of the mass of β-HCH in a certain volume of soil,[27] here we borrow and use this concept (mass center) to elucidate the change in geographical variation of the predicted soil residue of β-HCH with time. To evaluate the spatial variations of β-HCH soil residues on an annual basis from each individual scenario, a two-dimensional mass center of the soil residue (MCSR) of the chemical was introduced, given by

$$D_y = \frac{\sum_{j=1}^{ny}\sum_{i=1}^{nx}[M_{ij}\cdot(j-1)\cdot\Delta\theta\cdot\eta\cdot R]}{\eta\cdot R\cdot\sum_{j=1}^{ny}\sum_{i=1}^{nx}M_{ij}} = \frac{\Delta\theta\sum_{j=1}^{ny}\sum_{i=1}^{nx}[M_{ij}\cdot(j-1)]}{\sum_{j=1}^{ny}\sum_{i=1}^{nx}M_{ij}}$$

$$D_x = \frac{\sum_{j=1}^{ny}\sum_{i=1}^{nx}\{M_{ij}\cdot(i-1)\cdot\Delta\theta\cdot\eta\cdot R\cdot\cos[(j-0.5)\cdot\Delta\theta\cdot\eta]\}}{\eta\cdot R\cdot\cos(D_y\cdot\eta)\sum_{j=1}^{ny}\sum_{i=1}^{nx}M_{ij}} + 50.125$$

$$= \frac{\sum_{j=1}^{ny}\sum_{i=1}^{nx}\{M_{ij}\cdot(i-1)\cdot\Delta\theta\cdot\cos[(j-0.5)\cdot\Delta\theta\cdot\eta]\}}{\cos(D_y\cdot\eta)\sum_{j=1}^{ny}\sum_{i=1}^{nx}M_{ij}} + 50.125 \quad (1)$$

where D_y and D_x are latitude and longitude expressed in degrees, M_{ij} is soil residue mass of β-HCH at a grid cell (i, j), nx and ny are zonal and meridional grid number. $\Delta\theta$ is horizontal resolution of the model grid (= 0.25°). η and R are the ratio of radian to degree (=0.01745) and the mean radius of the Earth (=6371 km), respectively. A concept of the annual meridional displacement of MCSR was also used to highlight the spatial and temporal distribution of β-HCH soil residues associated with environmental factors. The displacement can be regarded as a vector, defined as the shortest distance between the end and starting positions of a MCSR and the moving direction of an object.[26] In our case, the displacement refers to as the shortest meridional distance between the MCSR for any adjacent two years, multiplied by the mean radius of the Earth. That is, $[D_y(n+1) - D_y(n)] \times \eta \times R$, where n is the number of years. The displacement >0 represents northward movement of a MCSR and <0 indicates the southward movement. To highlight mountain cold-trapping effect, we estimated wet scavenging ratio (W_T, dimensionless), which is the ratio of a chemical's concentration in precipitation to its concentration in air.[28] The W_T calculation considers that precipitation can scavenge organic chemicals from the atmosphere as vapors or particles (detailed in the SI). Hence, the W_T is the sum of the scavenging ratios for the vapor and for the particle-sorbed chemical. Since the W_T is a function of temperature, generally increasing with decreasing temperature and vice versa,[28] the ratio pictures the difference in the efficiency of precipitation scavenging driven by temperature, rather than the scavenging efficiency induced by change in precipitation rate with increasing altitude of a mountain. To assess the influence of precipitation on the scavenging efficiency, we assume that all wet deposition by the scavenging (W_T) occurs in the ABL. We also estimated a wet scavenging fraction (f_W), defined as the fraction of β-HCH mass scavenged by wet deposition to its total mass in the ABL, given by

$$f_W = \frac{W_T\zeta}{W_T\zeta + 1} \quad (2)$$

where ζ is the ratio of precipitation amount (m) to height of the ABL (1000 m).

Model Evaluation. The depth of surface soil for POPs soil sampling is often taken approximately at 20 cm. To evaluate the model performance, modeled β-HCH levels in the third soil layer (from 1.1 to 21.1 cm) derived from model scenario 1 were compared with available measured data of β-HCH soil concentrations across the model domain from 1975 to 2009, collected from literature (The data sources are listed in SI Table S5). SI Figure S5 highlights 80 sites where measured data (median and range) were available and used for the model evaluation, extracted from more than 5500 soil concentrations samples from literature. Since the sampling sites reported in literature were not defined accurately, here we adopted a simple method to compare modeled soil concentrations with those measurements. This method simply selects a rectangular area according to sampling areas described in literature. Details are described in the SI. Modeled maximum, minimum, and area-weighted soil concentrations at the third soil layer within a certain rectangular area were then compared with the corresponding measured concentrations within the rectangular area. The spearman rank correlation method was applied to assess model performance. This statistic is suitable for data with monotonic relationship and is insensitive to outliers. The t test statistics was used to assess significant level of the correlation analysis.

SI Table S5 lists detailed information of the measured and modeled data across the model domain for different periods at those sampling sites, as shown in SI Figure S5. SI Figure S6 is a scatter-plot of the measured median to modeled area-weighted soil concentrations. Although there are some large scatters, the modeled area-weighted and measured median concentrations exhibit a similar distribution. A Spearman correlation of 0.43 ($p < 0.005$, $n = 80$) between the two data sets suggests that the model captured to a large extent the temporal and spatial variations of β-HCH concentration in soil across the model domain. The median of the ratios of measured median concentrations to modeled area-weighted concentrations is 0.7. SI Figure S7 displays the frequency of the ratios after log-transformation. The transformed ratios indicate that 54% of modeled and measured concentrations are within 0.5 logarithmic unit and 86% within one logarithmic unit. This suggests that modeled concentration levels are comparable with the measured ones.[3]

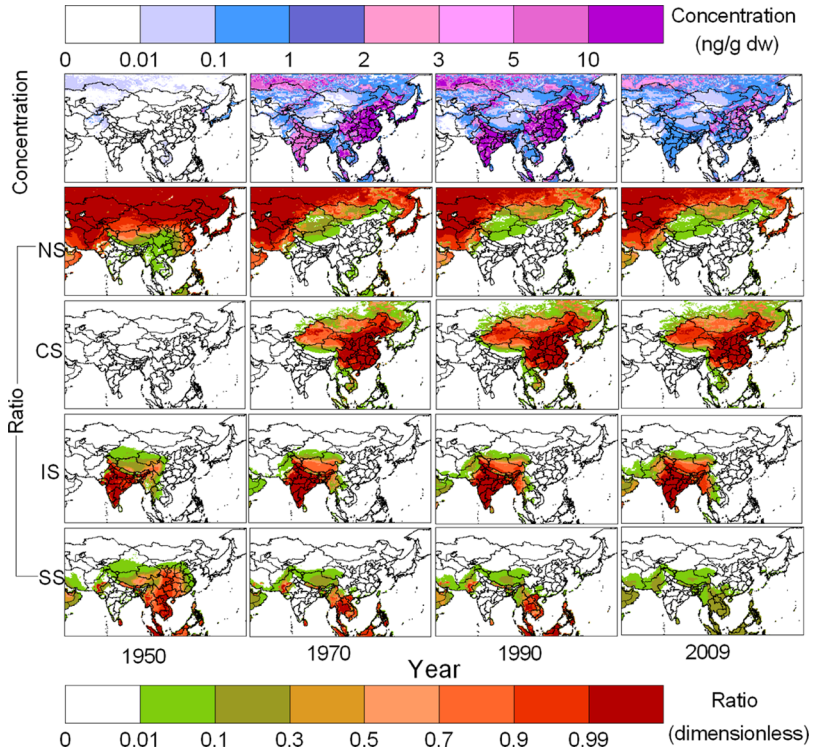

Figure 1. Modeled soil concentrations of β-HCH from the model scenario 1 (AS, top panel) and ratios of modeled soil concentrations from model scenarios 2−5 (considering individual source NS, CS, IS, and SS) to total soil concentrations summed over the model scenarios 2−5.

RESULTS AND DISCUSSION

Source Contribution. Figure 1 displays β-HCH soil residues in 1950, 1970, 1990, and 2009, derived from the model scenario 1, and the ratio of modeled soil concentrations from the four sources (NS, CS, IS and SS) to that from all sources in the model domain, defined by the model scenarios 2−5 respectively. Before 1952, technical HCH was used in the three source regions (NS, IS, and SS) in the model domain except China.[22] This enables us to investigate the influence of regional atmospheric circulation and wind pattern on the fate and redistribution of the chemical in the environment. This is done by examining β-HCH soil contamination in China and the contribution from the four sources to the spatial and temporal variation of the chemical. Before 1950, accumulated β-HCH usage in the NS region accounted for over 90% of the total use[22] and yielded dominant soil residues of β-HCH in the model domain in 1950. The East Asia summer monsoon and East Asia winter monsoon might play important roles in changes in the soil residues of β-HCH in northern and eastern areas of China (see text and Figure S8 in the SI). The use of β-HCH in both India and SS area accounted for 4% of the total usage in the model domain during 1948−1950, respectively.[22] This usage in India produced over 50% of soil residues in 1950 along the southeast boundary of the Tibetan Plateau. This high contribution ratio was strongly associated with the Indian summer monsoon, which carried high air concentrations of β-HCH from northwest India to the Tibetan Plateau, as shown in SI Figure S9. This has been demonstrated by previous analysis from sampled concentrations in air[13,14] and glaciers.[29] Due to significant wet deposition of β-HCH originated from India sources during the India monsoon season, and the influence of the extensive application of technical HCH in the NS region,[1,22] the India sources did not contribute considerably to the β-HCH contamination in northern China. Similarly, the SS also contributed a majority of soil residues to southern China in 1950. The spatial distribution of the contribution ratio from the SS to soil residues in China shows that there is an atmospheric transport route from the south to the north, characterized by a prevailing southerly wind which is a reflection of the typical pattern of the East Asia summer monsoon regime, as shown in SI Figure S10. Since the beginning of technical HCH use in China, soil residues of β-HCH in the four selected source regions were mostly dominated by their respective local emissions. The IS as an external source primarily contributed to soil residues in the Tibetan Plateau through atmospheric transport and deposition by the Indian summer monsoon. Another external source was the CS which contributed to soil residues in Mongolia through atmospheric transport and deposition by the East Asian summer monsoon.

Figure 2a shows measured β-HCH concentrations in a peat core and modeled total deposition (dry + wet deposition, from the model scenario 1) at the model grid where the peat core was sampled. The peat core was collected on May 24, 2006 at the Zoigê-Hongyuan bog (32°47′ N, 102°31′ E, see red trigon in SI Figure S5) in the northeast Tibetan Plateau. The detailed sampling and dating methods of the peat core have been described elsewhere[30] and are briefly summarized in the SI. As shown in Figure 2a, the temporal trend of modeled total deposition matches well with β-HCH concentration in the peat sample with a 3-year temporal resolution, as demonstrated by a Spearman correlation of 0.66 ($p < 0.005$) between the two data sets using the method for the model evaluation. Figure 2b displays the contribution from the four sources to the total deposition to the peat core sampling site, derived from the model scenarios 2−5. Among the four sources, the IS and SS made major contribution to the total deposition before

dx.doi.org/10.1021/es302017e | Environ. Sci. Technol. 2012, 46, 9525−9532

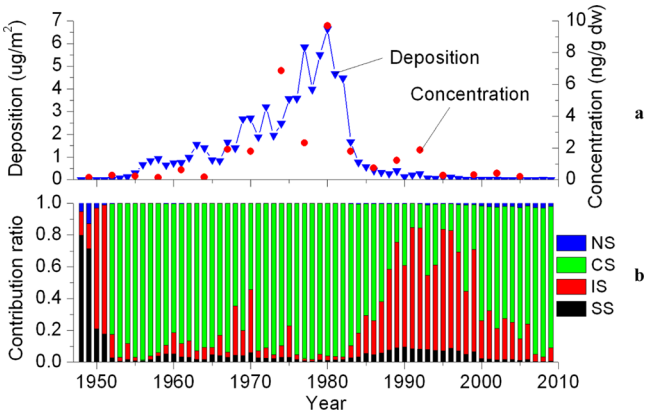

Figure 2. Measured β-HCH concentration in a peat core from Zoigê-Hongyuan, China and modeled total deposition (dry + wet deposition) at the model grid (a); Contribution of different sources to the deposition (b).

technical HCH was introduced in China, agreeing well with the source contribution to soil residues in the Tibetan Plateau as aforementioned. The CS mostly contributed to the deposition in the peat area during the application period of technical HCH in China. After 1984, when technical HCH was banned in China, the deposition to the peat area was mostly driven by the primary emission in the IS again. After 1999, when technical HCH was banned over the entire model domain and the reemission of the pesticide from previously contaminated soils became the main source, the secondary emission from the CS became a main contributor to the atmospheric deposition to the peat core sampling site, as shown in Figure 2b, because of the proximity of the peat core site to the CS.

Environmental Fate. The MCSR of β-HCH was defined as the weighted location of the mass of the pesticide averaged over a grid in the model domain (see the Materials and Methods section). By applying this concept, we can describe the spatial variation of soil residue of β-HCH on an annual basis in the model domain in terms of the movement of the MCSR from one place to another. The environmental processes related to the MCSR movement included in the model are primary and secondary emission of β-HCH, atmospheric transport and deposition, and degradation rate. Figure 3 illustrates annual β-HCH MCSR from 1948 to 2009 originating from the AS, NS, CS, IS, and SS, respectively. As aforementioned, accumulated β-HCH usage before 1950 was mainly in the NS region in the model domain, which resulted in the β-HCH MCSR in the northern area of the model domain. Following the increasing usage of the pesticide in China from 1952, the MCSR originated from the AS tended to merge with the MCSR from the CS owing to heavy application of technical HCH in the country.[4,22] After 1982, when the use of technical HCH was sharply decreased in China (see SI Figure S3), the MCSR from the AS extended westward, largely attributable to the use of technical HCH in India.[4] The movement of MCSR indicates that the primary emission mainly dominates the spatial pattern of β-HCH soil residues during the application period of technical HCH. After the ban of the pesticide over the entire model domain in 1999, all MCSRs shifted toward the north. The northward displacement of the MCSRs from the NS CS, IS, and SS followed the directions of wind components from these source regions in July as shown in SI Figure S4. This feature suggests that the Asian summer monsoon drove the northward delivery of β-HCH, as shown in SI Figures S9 and S10. This northward delivery contributed partly to the northward displacement of those MCSRs. On the other hand, slower degradation of β-HCH in northern cold regions as compared to southern warm areas (see SI Figure S12) also led to the higher soil residue in the north, marked by the northward shift of the MCSR. The northward movement of these MCSRs indicates that β-HCH residues in soil would increase with increase of Northern latitude and decrease of temperature, namely, the so-called cold condensation.[31]

We further computed annual meridional displacements of the MCSRs originated from the AS, NS, CS, IS, and SS from

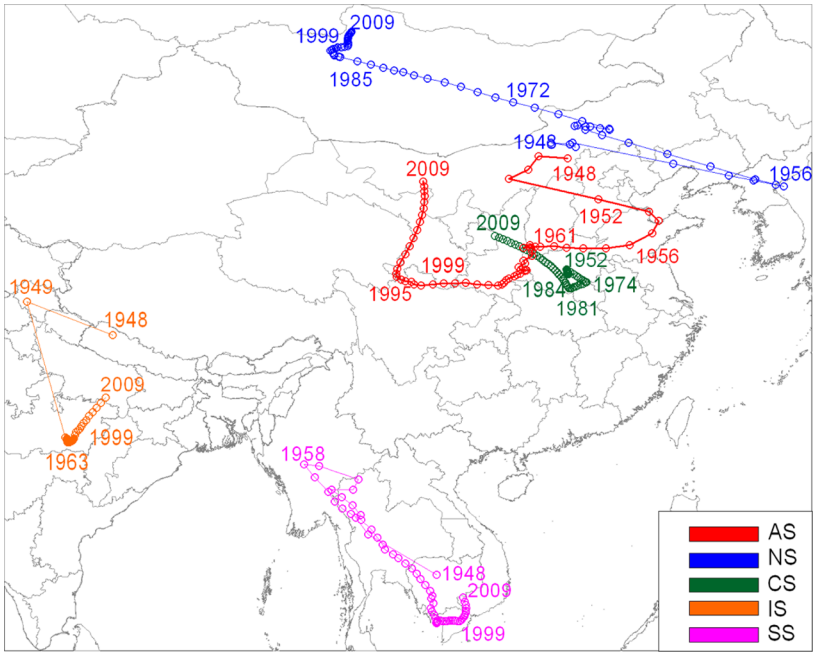

Figure 3. Displacement of mass centers of β-HCH soil residues during 1948–2009.

dx.doi.org/10.1021/es302017e | Environ. Sci. Technol. 2012, 46, 9525–9532

1999 to 2009, derived from the model scenarios 1 to 5, respectively. These displacements are displayed in SI Figure S13. The displacements of all MCSRs are positive, suggesting a northward movement of these MCSRs. This northward movement indicates relative enrichment of soil residues of β-HCH in the cold northern area compared with that in warm southern area. The meridional MCSR displacement during 1999−2009 from the AS, NS, and CS shows a downward trend at a 95% confidence level from the t test statistics. This downward trend indicates that decreasing temperature with the relative enrichment of β-HCH toward the northern area (see SI Figure S11) can lock more mass and slow down degradation and reemission. This can be regarded as an underlying signal of cold condensation. Whereas the linear trends of meridional MCSR displacements away from the IS and SS are positive at a 99% confidence level from the t test statistics, indicating faster northward movement of the MCSRs from the two sources. This result cannot be explained by cold condensation effect. Rather, it is related to the (Tibetan Plateau) mountain cold trapping,[28] as will be elaborated below.

Cold Trapping Effect of Tibetan Plateau. As aforementioned, the IS and SS mainly contributed to the β-HCH contamination in the Tibetan Plateau. Figure 4a and SI Figure S14 show the soil residues in 2009, originated from the IS and SS, respectively. The spatial patterns of the soil residues in the Tibetan Plateau from the IS and SS were similar, suggesting similar environmental processes that favor the accumulation of the pesticide in the plateau soil, transported from these two sources. The residue levels from the IS were higher than those from the SS. Therefore, the present analysis will focus on the IS contribution to the soil residues in the plateau and corresponding environmental factors, in order to elucidate the mechanisms of β-HCH accumulation and contamination in the Tibetan Plateau.

Figure 4b displays the cross sections of soil concentration in 2009, terrain height, annual mean temperature, and precipitation rate during 2000−2009, extending from 7.5 to 32.5 °N, averaged over longitude 72.5−92.5 °E (see blue box in Figure 4a). As seen, the terrain height rises sharply from 27 °N on the southern slope of the plateau, resulting in rapid decrease of temperature and precipitation rate. The precipitation rate appears to exhibit a slower declining trend with terrain height as compared with temperature trend because of orographic effects.[28] Mountain cold-trapping refers to the relative enrichment of some semivolatile organic compounds at higher altitudes as a result of temperature controlled environmental partitioning processes. Wet deposition processes are efficient in transferring organic contaminants from the atmosphere to the Earth's surface, if their W_T is within the range between two thresholds ($3.5 < \log W_T < 5.5$, termed as Wet Scavenging Ratio Relevance Range, WRR) with change in temperature.[28] To examine the connection between the atmospheric deposition of β-HCH and temperature and precipitation rate, we estimated the W_T and f_W of β-HCH from atmosphere (see the Materials and Methods section) using the temperature and precipitation rate shown in Figure 4b. The difference of the scavenging efficiency between rain and snow was not taken into consideration in the present study because the W_T of β-HCH at 0 °C is comparable to that at −10 °C,[32] and the transport and deposition from main β-HCH source region to areas with higher altitudes are primarily by Indian monsoon and East Asian monsoon in summer, when rain is major form of precipitation. Result is presented in SI Figure S15. Although the

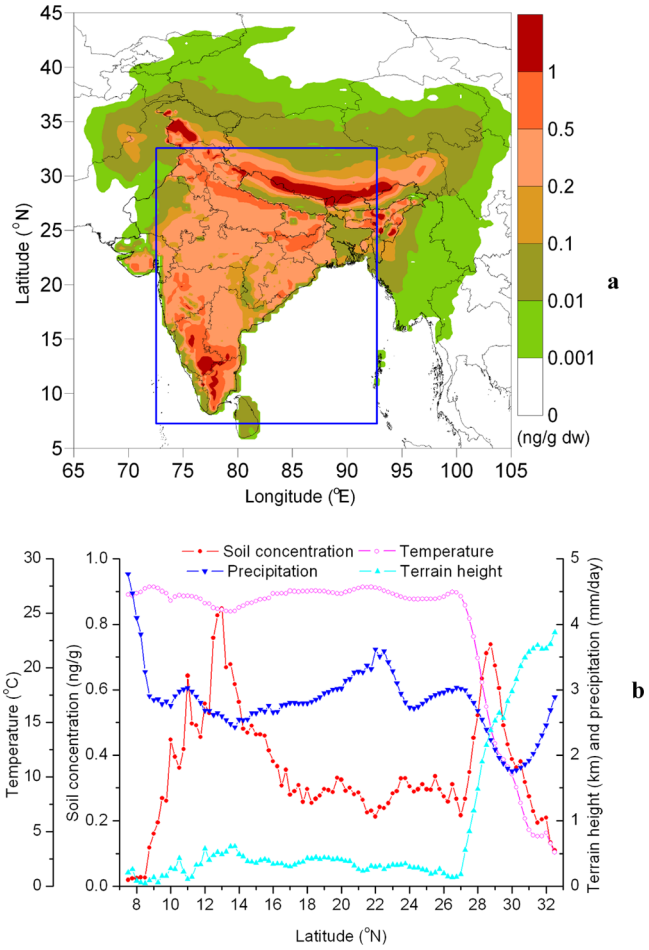

Figure 4. Soil residues of β-HCH in 2009 originated from the Indian source. The blue box is a region extending from 7.5 to 32.5 °N and from 72.5 to 92.5 °E, which is used to assess cold trapping effect (a); Cross sections of soil concentration in 2009, terrain height, and annual mean temperature and precipitation rate during 2000 − 2009 extending from 7.5 to 32.5 °N averaged over longitude 72.5−92.5 °E as shown the blue box in Figure 4a (b).

W_T (~4.8 of log W_T) is in the range of WRR in the south of 27°N, the f_W suggests that only ~15% of β-HCH in the air compartment of the ABL (below 1000 m height) is scavenged by wet deposition. With the increase of the terrain height from 27 °N to the north, the W_T and f_W rise sharply. The f_W shows that 30% of β-HCH in the ABL can be scavenged by wet deposition near 29 °N, where the log W_T is about 5.3 and the soil residues of β-HCH reach a peak (see Figure 4b). The W_T increases sequentially and exceeds the upper limit of threshold values of the WRR from the north of 30 °N, where the wet deposition rate is no longer sensitive to the value of W_T.[28] In the region between 29 and 30 °N, the W_T is also within the WRR but modeled soil residues of β-HCH decrease sharply. This suggests that in this case the W_T is only related to temperature and significant influence of precipitation on the deposition. Intriguingly, the f_W keeps ~30% over 29−30 °N. This suggests that 30% of f_W may be taken as a threshold while assessing wet deposition rate. Previous studies have also found that sampled β-HCH concentrations in fish[33] and conifer needles[34] were higher near 29 °N than that in the northern areas of the plateau. These results indicate that the geographical pattern of β-HCH soil residues in the Tibetan Plateau from the

dx.doi.org/10.1021/es302017e | Environ. Sci. Technol. 2012, 46, 9525−9532

IS is very likely resulted from the wet deposition due to effective precipitation scavenging, or the mountain cold trapping effect,[28] along the southern slope of the plateau. Previous analysis for soil samples collected from the Tibetan Plateau has revealed the cold trapping of POPs along the East-slope of the plateau.[12] The SS in the model scenario 5 refers to the β-HCH use in South Asian countries (excluding India), including Nepal[35] and Pakistan,[36] and Southeast Asian countries. β-HCH contamination to the Tibetan Plateau from the SS is therefore largely related to the interaction of atmospheric transport from the SS and mountain cold trapping effect over South- and East-slopes of the plateau. As a result, the northward displacement of MCSR from the IS and SS should have contained a signal of the cold trapping effect of the plateau.

As shown in Figure 4b, soil concentration of β-HCH increases from 1000 m terrain height toward northern higher mountain, reaching a peak at terrain height near 4000 m due to the mountain cold trapping effect. This implies that we could identify the cold-trapping signal from calculated displacements of the MCSR by excluding soil residues of β-HCH at different terrain height. To further elucidate potential mountain cold trapping effect, we first removed the soil residues of β-HCH from 1000 and 5000 m terrain height, respectively. For the former case, this is equivalent to removing accumulated soil burden of β-HCH in the Tibetan Plateau potentially caused by cold trapping effect over the Plateau or "removing" the Plateau, thereby addressing the Plateau cold trapping effect. We then recalculated the meridional displacement of MCSR away from the IS and SS. Results are displayed in SI Figure S16 and Figure S17, respectively. For the case of excluding soil residues of β-HCH above 1000 m terrain height, the annual displacements of the MCSR from the both sources are almost entirely negative during 1999−2009, indicating southward displacement of the MCSR. The southward displacement can be attributed to the accumulation of β-HCH in south Deccan Plateau of India (see Figure 4a), and Indonesia and Malaysia (see SI Figure S14). These areas have relatively high terrain (see SI Figure S4) and low temperature (see SI Figure S11), which favors β-HCH accumulation in the soil. Differing from the positive linear trends of the MCSR displacements with 99% confidence level as shown in SI Figure S13, the southward displacements of the MCSR from the IS and SS, after removing the soil residues above 1000 m terrain height, show weakly positive and negative trend which are not statistical significant from the t test statistics, implying relatively weaker or insignificant mountain cold trapping effect over these relatively lower mountain areas, for example, southern Deccan Plateau of India. On the other hand, the linear trends of the MCSR displacements from IS (SI Figure S16) and SS (SI Figure S17), after removing β-HCH soil residues from above 5000 m terrain height, are positive at a 99% confidence level from the t test statistics, further demonstrating that the faster northward displacement of the MCSR from these two sources can be attributed to the cold trapping effect of the Tibetan Plateau.

In summary, this modeling investigation assessed the environmental fate and source-receptor relationships of β-HCH before and after the phase-out of technical HCH over Asia, and its association with environmental factors. Results presented here demonstrated that Indian monsoon and East Asian monsoon in summer dominated the northward delivery of β-HCH from India source, and Southeast Asia and China source, respectively. The environmental fate of β-HCH from China and the rest of Northeast Asian countries and regions can be overall explained by cold condensation, whereas the environmental fate of β-HCH from India and Southeast Asian countries and regions are subject to cold trapping effect of the Tibetan Plateau. Given that the developing countries in Asia, such as India, China and Southeast countries have been considered as main source region of many POPs, such as endosulfan, DDT, and PAHs, the environmental behaviors of those chemicals having similar physicochemical properties as β-HCH would likely to be also driven by similar environmental factors. Results presented here will help to improve our understanding to the potential impacts of environmental factors on the fate and source-receptor relationship of POPs, and provide further support to recent international efforts in effective elimination of POPs.

■ ASSOCIATED CONTENT

Supporting Information

Additional material as noted in the text. This material is available free of charge via the Internet at http://pubs.acs.org.

■ AUTHOR INFORMATION

Corresponding Author

*Phone: +86-535-2109-160; fax: +86-535-2109-000; e-mail: cgtian@yic.ac.cn.

Notes

The authors declare no competing financial interest.

■ ACKNOWLEDGMENTS

This work was supported by the Knowledge Innovation Program of the Chinese Academy of Sciences (Nos. KZCX2-YW-GJ02 and KZCX2-YW-QN210), the Promotive Research Foundation for Excellent Young and Middle-Aged Scientists of Shandong Province (No. BS2012HZ028), and the Natural Scientific Foundation of China (Nos. 41101495 and 41125014). The authors gratefully acknowledge Global Soil Data Task and National Centers for Environmental Prediction for providing environmental data.

■ REFERENCES

(1) Li, Y. Global technical hexachlorocyclohexane usage and its contamination consequences in environment: From 1947 to 1997. *Sci. Total Environ.* **1999**, *232*, 123−160.

(2) Willett, K.; Ulrich, E.; Hites, R. Differential toxicity and environmental fates of hexachlorocyclohexane isomers. *Environ. Sci. Technol.* **1998**, *32*, 2197−2207.

(3) Wöhrnschimmel, H.; Tay, P.; von Waldow, H.; Hung, H.; Li, Y.-F.; MacLeod, M.; Hungerbühler, K. Comparative assessment of the global fate of α- and β-hexachlorocyclohexane before and after phase-out. *Environ. Sci. Technol.* **2012**, *46* (4), 2047−2054.

(4) Li, Y.; Macdonald, R. Sources and pathways of selected organochlorine pesticides to the Arctic and the effect of pathway divergence on HCH trends in biota: A review. *Sci. Total Environ.* **2005**, *342* (1−3), 87−106.

(5) Liu, X.; Zhang, G.; Li, J.; Yu, L.; Xu, Y.; Li, X.; Kobara, Y.; Jones, K. C. Seasonal patterns and current sources of DDTs, chlordanes, hexachlorobenzene, and endosulfan in the atmosphere of 37 Chinese cities. *Environ. Sci. Technol.* **2009**, *43* (5), 1316−1321.

(6) Zhang, G.; Chakraborty, P.; Li, J.; Sampathkumar, P.; Balasubramanian, T.; Kathiresan, K.; Takahashi, S.; Subramanian, A.; Tanabe, S.; Jones, K. C. Passive atmospheric sampling of organochlorine pesticides, polychlorinated biphenyls, and polybrominated diphenyl ethers in urban, rural, and wetland sites along the coastal length of India. *Environ. Sci. Technol.* **2008**, *42* (22), 8218−8223.

(7) Yu, Y.; Tao, S.; Liu, W.; Lu, X.; Wang, X.; Wong, M. Dietary intake and human milk residues of hexachlorocyclohexane isomers in two Chinese cities. *Environ. Sci. Technol.* **2009**, *43* (13), 4830−4835.
(8) Abhilash, P.; Singh, N. Seasonal variation of HCH isomers in open soil and plant-rhizospheric soil system of a contaminated environment. *Environ. Sci. Pollut. Res.* **2009**, *16* (6), 727−740.
(9) Chen, D.; Zhang, X.; Mai, B.; Sun, Q.; Song, J.; Luo, X.; Zeng, E. Y.; Hale, R. C. Polychlorinated biphenyls and organochlorine pesticides in various bird species from northern China. *Environ. Pollut.* **2009**, *157* (7), 2023−2029.
(10) Su, Y.; Wania, F.; Lei, Y. D.; Harner, T.; Shoeib, M. Temperature dependence of the air concentrations of polychlorinated biphenyls and polybrominated diphenyl ethers in a forest and a clearing. *Environ. Sci. Technol.* **2007**, *41* (13), 4655−4661.
(11) Ma, J.; Li, Y. F. Interannual variation of persistent organic pollutants over the Great Lakes induced by tropical Pacific sea surface temperature anomalies. *J. Geophys. Res.* **2006**, *111*, D04302 DOI: 10.1029/2005JD006014.
(12) Chen, D.; Liu, W.; Liu, X.; Westgate, J. N.; Wania, F. Cold-trapping of persistent organic pollutants in the mountain soils of Western Sichuan, China. *Environ. Sci. Technol.* **2008**, *42* (24), 9086−9091.
(13) Wang, X.-p.; Gong, P.; Yao, T.-d.; Jones, K. C. Passive air sampling of organochlorine pesticides, polychlorinated biphenyls, and polybrominated diphenyl ethers across the Tibetan Plateau. *Environ. Sci. Technol.* **2010**, *44* (8), 2988−2993.
(14) Gong, P.; Wang, X.; Sheng, J.; Yao, T. Variations of organochlorine pesticides and polychlorinated biphenyls in atmosphere of the Tibetan Plateau: Role of the monsoon system. *Atmos. Environ.* **2010**, *44* (21−22), 2518−2523.
(15) Tian, C.; Ma, J.; Liu, L.; Jia, H.; Xu, D.; Li, Y. A modeling assessment of association between East Asian summer monsoon and fate/outflow of α-HCH in Northeast Asia. *Atmos. Environ.* **2009**, *43* (25), 3891−3901.
(16) Tian, C.; Liu, L.; Ma, J.; Tang, J.; Li, Y. Modeling redistribution of α-HCH in Chinese soil induced by environment factors. *Environ. Pollut.* **2011**, *159* (10), 2961−2967.
(17) Tian, C.; Ma, J.; Chen, Y.; Liu, L.; Ma, W.; Li, Y.-F. Assessing and forecasting atmospheric outflow of α-HCH from China on intra-, inter-, and decadal time scales. *Environ. Sci. Technol.* **2012**, *46* (4), 2220−2227.
(18) Wania, F.; Mackay, D. A global distribution model for persistent organic chemicals. *Sci. Total Environ.* **1995**, *160/161*, 211−232.
(19) Kalnay, E.; Kanamitsu, M.; Kistler, R.; Collins, W.; Deaven, D.; Gandin, L.; Iredell, M.; Saha, S.; White, G.; Woollen, J.; Zhu, Y.; Leetmaa, A.; Reynolds, B.; Chellia, M.; Ebisuzaki, W.; Higgins, W.; Janowiak, J.; Mo, K.; Ropelewski, C.; Wang, J.; Jenne, R.; Joseph, D. The NCEP/NCAR reanalysis project. *Bull. Am. Meteorol. Soc.* **1996**, *77*, 437−471.
(20) Friedl, M. A.; McIver, D. K.; Hodges, J. C. F.; Zhang, X. Y.; Muchoney, D.; Strahler, A. H.; Woodcock, C. E.; Gopal, S.; Schneider, A.; Cooper, A.; Baccini, A.; Gao, F.; Schaaf, C. Global land cover mapping from MODIS: Algorithms and early results. *Remote Sens. Environ.* **2002**, *83* (1−2), 287−302.
(21) *Global Soil Data Task. Global Gridded Surfaces of Selected Soil Characteristics (IGBPDIS). International Geosphere-Biosphere Programme—Data and Information Services*; Oak Ridge National Laboratory: Oak Ridge, TN, http://www.daac.ornl.gov/ (accessed July 1, 2002).
(22) Li, Y. Global gridded technical hexachlorocyclohexane usage inventory using a global cropland as a surrogate. *J. Geophys. Res.* **1999**, *104* (D19), 23785−23797.
(23) Li, Y.; Scholtz, M. T.; Van Heyst, B. J. Global gridded emission inventories of β-Hexachlorocyclohexane. *Environ. Sci. Technol.* **2003**, *37* (16), 3493−3498.
(24) He, Q.; Zhou, G. The climatic suitability for maize cultivation in China. *Chin. Sci. Bull.* **2012**, *57* (4), 395−403.
(25) Klemann, V.; Martinec, Z. Contribution of glacial-isostatic adjustment to the geocenter motion. *Tectonophysics* **2011**, *511* (3−4), 99−108.
(26) Maus, H. M.; Seyfarth, A.; Grimmer, S. Combining forces and kinematics for calculating consistent centre of mass trajectories. *J. Exp. Biol.* **2011**, *214* (21), 3511−3517.
(27) Tao, S.; Liu, W.; Li, Y.; Yang, Y.; Zuo, Q.; Li, B.; Cao, J. Organochlorine pesticides contaminated surface soil as reemission source in the Haihe Plain, China. *Environ. Sci. Technol.* **2008**, *42* (22), 8395−8400.
(28) Wania, F.; Westgate, J. N. On the mechanism of mountain cold-trapping of organic chemicals. *Environ. Sci. Technol.* **2008**, *42* (24), 9092−9098.
(29) Wang, X.-p.; Yao, T.-d.; Wang, P.-l.; Wei, Y.; Tian, L.-d. The recent deposition of persistent organic pollutants and mercury to the Dasuopu glacier, Mt. Xixiabangma, central Himalayas. *Sci. Total Environ.* **2008**, *394* (1), 134−143.
(30) Shi, W.; Feng, X.; Zhang, G.; Ming, L.; Yin, R.; Zhao, Z.; Wang, J. High-precision measurement of mercury isotope ratios of atmospheric deposition over the past 150 years recorded in a peat core taken from Hongyuan, Sichuan Province, China. *Chin. Sci. Bull.* **2011**, *56* (9), 877−882.
(31) Wania, F.; Mackay, D. Tracking the distribution of persistent organic pollutants. *Environ. Sci. Technol.* **1996**, *30* (9), 390A−396A.
(32) Lei, Y. D.; Wania, F. Is rain or snow a more efficient scavenger of organic chemicals? *Atmos. Environ.* **2004**, *38* (22), 3557−3571.
(33) Yang, R.; Yao, T.; Xu, B.; Jiang, G.; Xin, X. Accumulation features of organochlorine pesticides and heavy metals in fish from high mountain lakes and Lhasa River in the Tibetan Plateau. *Environ. Int.* **2007**, *33* (2), 151−156.
(34) Yang, R.; Yao, T.; Xu, B.; Jiang, G.; Zheng, X. Distribution of organochlorine pesticides (OCPs) in conifer needles in the southeast Tibetan Plateau. *Environ. Pollut.* **2008**, *153* (1), 92−100.
(35) Atreya, K. Pesticide use knowledge and practices: A gender differences in Nepal. *Environ. Res.* **2007**, *104* (2), 305−311.
(36) Tariq, M. I.; Afzal, S.; Hussain, I.; Sultana, N. Pesticides exposure in Pakistan: A review. *Environ. Int.* **2007**, *33* (8), 1107−1122.